

On-line determination of transient stability status using multilayer perceptron neural network

Emmanuel Asuming Frimpong^{*}, Philip Yaw Okyere^{*},
Johnson Asumadu^{**}

A scheme to predict transient stability status following a disturbance is presented. The scheme is activated upon the tripping of a line or bus and operates as follows: Two samples of frequency deviation values at all generator buses are obtained. At each generator bus, the maximum frequency deviation within the two samples is extracted. A vector is then constructed from the extracted maximum frequency deviations. The Euclidean norm of the constructed vector is calculated and then fed as input to a trained multilayer perceptron neural network which predicts the stability status of the system. The scheme was tested using data generated from the New England test system. The scheme successfully predicted the stability status of all two hundred and five disturbance test cases.

Key words: power system stability, stability prediction, transient stability, out-of-step, neural network, Euclidean norm

1 Introduction

The demand for electric power keeps on growing. This is making power companies to push more power through existing transmission lines resulting in operations with reduced stability margins. Additionally, system stability limits are changing due to the integration of renewable energy sources [1]. Large disturbances occurring in systems operating with reduced stability margins may lead to out-of-step (OS) conditions between generators or generator groups. OS conditions are usually characterized by large separation of generator rotor angles, large swings of power flows and large fluctuations of voltage and current [2]-[3]. They eventually result in system failure and equipment damage if there is no appropriate remedial action.

Electric power companies are required to maintain high levels of reliability of electricity supply. It is therefore imperative that adequate measures are put in place to prevent OS conditions. Possible measures that can be adopted are: out-of-step blocking and tripping, fast-valve control of turbines, dynamic braking, use of superconducting magnetic energy storage system, system switching, modulation of high voltage direct current (HVDC) link power flow, and controlled islanding with load shedding [4]. The effectiveness of these measures will be greatly enhanced if out-of-step conditions can be detected early.

Researchers have proposed a number of schemes for detecting transient instability [4-14]. These schemes have

used power system input data such as rotor angle [4-10], bus voltage [10-14], mechanical input power [7,13], electromagnetic power [7,13], line current [11,14], generator frequency [10] and rotor speed [9]. Decision making tools such as artificial neural network [4], fuzzy logic [14], support vector machine [7,10] and decision trees [9,14] have also been employed. Although significant successes have been chalked, improvements are still required in the areas of simplicity, reliability, speed of operation and practical realization. For example, the work presented in [8] requires 10-12 input data samples per generator which makes the volume of data required for large systems huge and consequently delays the response time of the scheme. Again in [7], thirty four input features are constructed from generator variables. The work in [9] also requires a relatively long period of up to 2.5 seconds after fault clearance to make a decision as to whether the system will be stable or not. The schemes proposed in [10], [12] use predetermined templates which make their performance susceptible to changes in system conditions. Furthermore, the technique presented in [5] also uses predetermined stability boundary for each generator, and its application to real systems requires extensive dynamic simulations to establish the stability boundaries.

This paper attempts to address these outstanding issues. It presents a simple, highly accurate, speedy and easy to implement technique for predicting the stability status of power systems following a disturbance. It uses generator bus frequency deviations sampled at a sampling

^{*} Department of Electrical and Electronic Engineering, Kwame Nkrumah University of Science and Technology, Kumasi, Ghana, eafrimpong.soe@knust.edu.gh, ^{**} Department of Electrical and Computer Engineering, Western Michigan University, Kalamazoo, USA

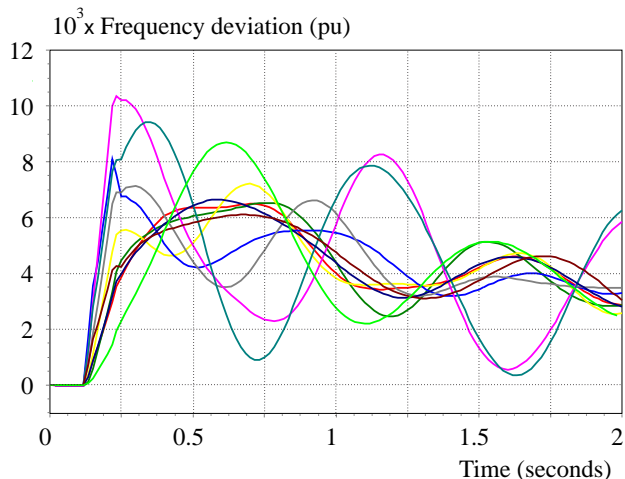


Fig. 1. Machine terminal frequency deviations for a stable condition

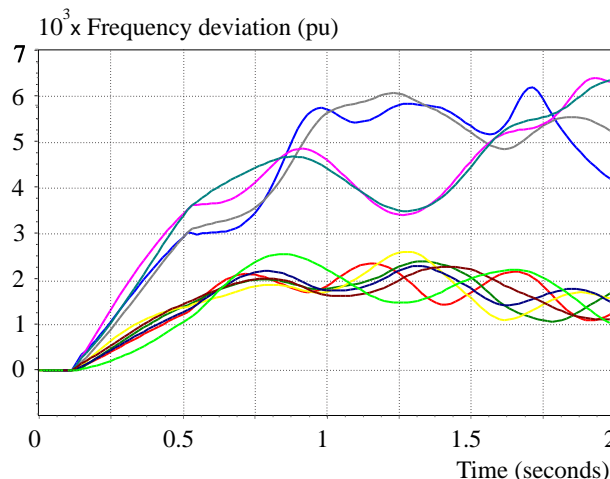


Fig. 2. Machine terminal frequency deviations for an unstable condition

frequency of 60 samples per second as input data. This sampling frequency is a typical sampling rate of phasor measurement units [15]. Only the first two samples of frequency deviations at each generator bus are required. From the sampled frequency deviations, the maximum frequency deviation is obtained for each generator. The Euclidean norm of a vector with these maximum frequency deviations as elements is calculated. The calculated norm is then fed into a trained multilayer perceptron neural network (MLPNN) which predicts the stability status. The MLPNN gives an output of 0 if the system will be transient stable and an output of 1 if transient instability will occur.

2 Machine terminal frequency deviation as input parameter

Generator bus frequencies like rotor angles swing following a power system disturbance. For a stable system, the bus frequency of all generators may increase or decrease but will eventually settle at a synchronous value. The rates of increase or decrease are all reduced. On the other hand, for a condition leading to instability, the bus frequency of one or more generators will increase or decrease progressively with higher amplitudes.

Figures 1 and 2 show curves of generator frequency deviations for a three-phase fault on the line between buses 16 and 21 of the test system shown in Fig. 5. These curves were obtained through dynamic simulations using the Power System Simulator for Engineers (PSSE) software [16]. Figure 1 is for the case where the fault lasted for 100 ms resulting in transient stability and Fig. 2 is for the case where the fault lasted for 400 ms resulting in transient instability. As was expected, the bus frequencies in Fig. 1 increased but later showed signs of stabilising. On the other hand, the bus frequencies of some of the generators in Fig. 2 increased progressively. The curves in

figures 1 and 2 show that it is possible to use the trajectories of bus frequency deviations following a disturbance to predict whether a system will be stable.

3 Multilayer perceptron neural network as decision making tool

Artificial neural networks (ANNs) are decision making tools that have been widely used in power system studies. There are different kinds of ANNs. Multilayer perceptron neural networks (MLPNNs) are one of the commonly used types. MLPNNs can be used for both function fitting and pattern recognition problems. They can also be used for prediction problems. MLPNNs are an interconnection of artificial neurons (with or without biases) with each neuron having an activation (or transfer) function [17]. The transfer functions influence the outputs of the neurons. Commonly used transfer functions are: linear, tan-sigmoid, and log-sigmoid [17,18]. The neurons are organised in layers, namely input layer, hidden layer (s) and output layer. MLPNNs work by taking an input signal vector and propagating it to the input layer neurons through connections with weights. The outputs of the input layer neurons (determined by their activation functions) become the inputs to the hidden layer neurons. These new inputs are also propagated through weighted connections to the hidden layer neurons. The outputs of the hidden layer neurons are finally propagated to the output layer where the final output of the network is produced. The weights of the connections are determined in a training process where the neural network is presented with input-output pairs. A training algorithm is employed to adjust the weights until a desired outcome is reached. ANNs can be implemented using the MATLAB software [17]. Figure 3 shows the architecture of the MLPNN used. The variable x is the input data, w_{ij} is the weight between neurons i and j , w_{i0} is the weight of the bias of neuron i , and O is the output of the neural network. The input neuron has a linear transfer function

while the hidden layer and output neurons have tangent sigmoid transfer functions.

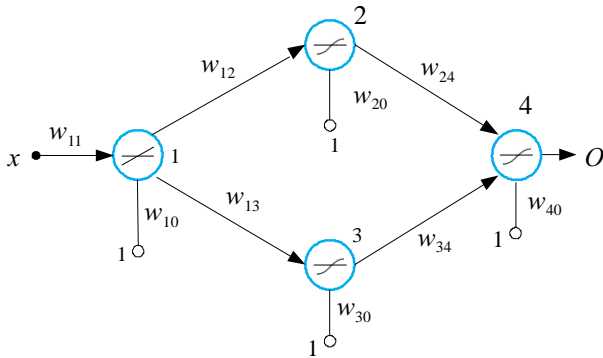


Fig. 3. Architecture of used MLPNN

The output, y_1 , of neuron 1 is given by

$$y_1 = f(xw_{11} + w_{10}) = xw_{11} + w_{10} \quad (1)$$

The output, y_2 , of neuron 2 is given by

$$y_2 = f(y_1w_{12} + w_{20}) = \frac{e^{2(y_1w_{12} + w_{20})} - 1}{e^{2(y_1w_{12} + w_{20})} + 1} \quad (2)$$

The output, y_3 , of neuron 3 is given by

$$y_3 = f(y_1w_{13} + w_{30}) = \frac{e^{2(y_1w_{13} + w_{30})} - 1}{e^{2(y_1w_{13} + w_{30})} + 1} \quad (3)$$

The output, O , of MLPNN is thus given by

$$O = f(y_2w_{24} + y_3w_{34} + w_{40}) \quad (4)$$

Hence,

$$O = \frac{e^{2(y_2w_{24} + y_3w_{34} + w_{40})} - 1}{e^{2(y_2w_{24} + y_3w_{34} + w_{40})} + 1} \quad (5)$$

The MLPNN was trained to give an output of either 0 or 1 using the Levenberg-Marquardt training algorithm. It is one of the most efficient training algorithms [17]. An output of 0 indicates that the system will be transient stable, while an output of 1 indicates imminent transient instability.

In practice, neural networks do not always give exact outputs of 0 or 1. For example, an expected 0 value may be presented as -0.015 while an expected value of 1 may be presented as 0.95. As a result, in this work, (6) and (7) are used to round the outputs of the MLPNN to either 0 or 1.

$$O \geq 0.5 \rightarrow O = 1 \quad (6)$$

$$O < 0.5 \rightarrow O = 0 \quad (7)$$

4 Proposed method for predicting transient stability status

Figure 4 shows a functional block diagram of the proposed technique. The proposed scheme uses the frequency deviations at generator buses as input data. The input data is obtained and processed using the procedure outlined below.

Sample frequency deviations at all generator buses using a sampling frequency of 60 samples per second. For each generator bus, only the first two samples are required. The first two samples for each generator bus was found to be the optimal number of samples for the scheme. Thus, the sampled frequency deviations, f_n , at generator bus n is given as

$$f_n = \{f_{1,n}, f_{2,n}\}, \quad n = 1, 2, 3, \dots, N \quad (8)$$

where N is the number of generator buses of the system.

For each f_n , determine the maximum deviation

$$f_{n,\max} = \text{Max}(f_n). \quad (9)$$

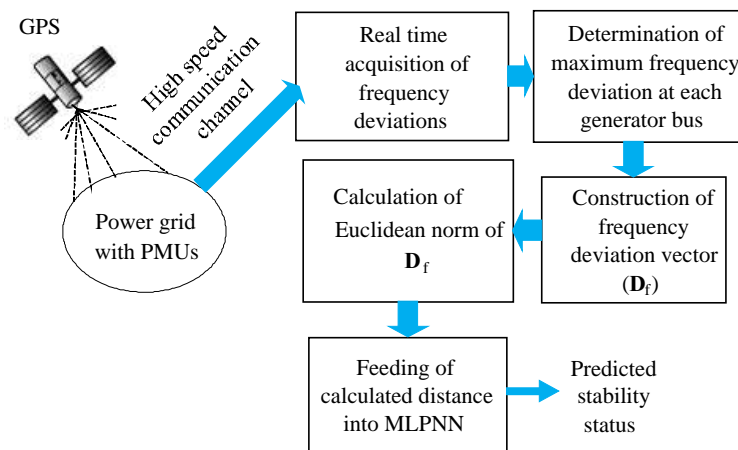


Fig. 4. Functional block diagram of the proposed technique

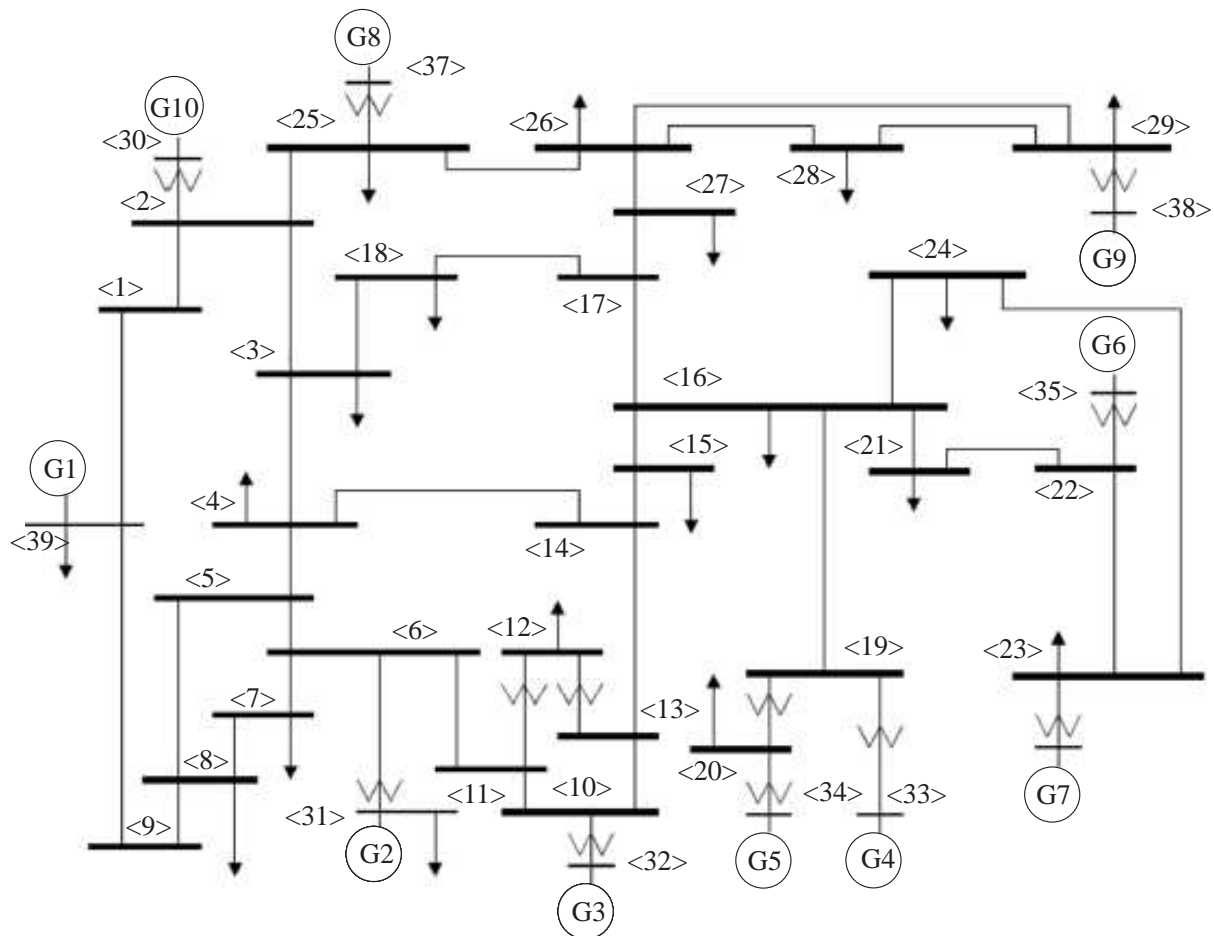


Fig. 5. IEEE 39 - bus test system

Construct the frequency deviation vector

$$D_f = [f_{1,max} \quad f_{2,max} \quad \dots \quad f_{N,max}] \quad (10)$$

Determine the Euclidean norm, d , of the frequency deviation vector

$$d = \sqrt{f_{1,max}^2 + f_{2,max}^2 + \dots + f_{N,max}^2} \quad (11)$$

Feed obtained Euclidean norm into trained MLPNN to obtain predicted stability status. That is put $x = d$ in (1) to (5).

5 Test system and simulations

Development and testing of the proposed scheme was done using the IEEE 39-bus test system which is also known as the New England test system. This test system is a standard test system widely used for small and large signal stability studies [2,4,5,10,12]. The system consists of 10 generators, one of which is a generator representing a large system. The system is shown in Fig. 5.

Transient stability analysis of the test system was performed using the PSSE software [16]. A detailed dynamic

model which includes prime mover and excitation system dynamics was used. Several fault simulations were obtained by varying the following: (i) fault location, (ii) fault duration, (iii) system loading, (iv) network topology, and (v) generator availability.

As regards fault location, bus and line faults at different locations were simulated. Fault durations were also varied by starting with short durations which resulted in transient stability and extending them gradually until instability occurred. The loading conditions simulated were base load, 80% of base load, 90% of base load, 110% of base load and 120% of base load. The effect of shutting down a generator due to low loading conditions or for purposes of maintenance was also considered. For example, for a loading level of 80% base load, generator 10 (G10) was removed from circuit before disturbances were applied. Additionally, the effect of changes in network topology was investigated by considering N-1 contingency. For example, for some of the simulations, the line between bus 18 and bus 17 was removed before the application of faults.

A total of two hundred and nine three-phase bus and line faults were simulated. One hundred and four of the faults simulated resulted in transient stability while the remaining 105 resulted in transient instability. Frequency

deviation data from four fault conditions comprising 2 unstable fault cases and 2 stable cases were used to train the MLPNN. The remaining 205 fault cases were used to test the MLPNN. Thus only 1.91% of data generated was used for training the MLPNN. Compared with existing schemes in literature, such as in [2] which used 75% of total generated data for training, the training data used in the proposed scheme is very low. Such a low volume of training data will make simple, the application of this technique to real systems with large number of generators. The low volume of data used to train the MLPNN was made possible due to the fact that the calculated Euclidean norm values, d , for stable cases were so distinct from those of unstable cases. This goes to show the strength of the proposed technique over existing ones.

6 Results and analysis

6.1 Architecture of trained neural network

Figure 6 shows the architecture of the neural network (with obtained weight values) after training using Euclidean norm data obtained from the four fault cases. The fault cases were: (i) 1 stable fault condition on the line between buses 2 & 25, and 1 unstable fault condition on the same line, all at 120% base loading, and (ii) 1 stable and 1 unstable fault condition on the line between buses 22 & 23 at 110% base loading. The training data as presented in MATLAB is given as follows:

Input data = [0.0071 0.0034 0.057 0.0551],

Target data = [0 0 1 1]

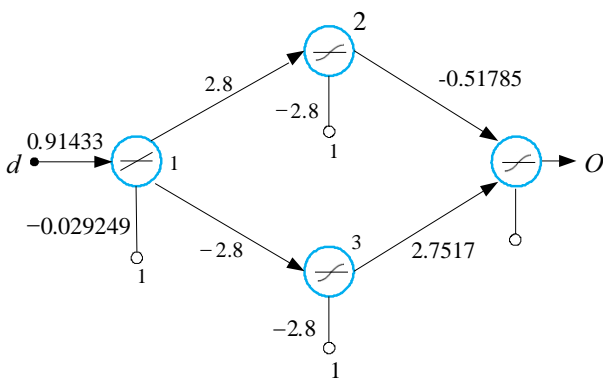


Fig. 6. Architecture of trained MLPNN

It is important to note that the neural network training process in MATLAB involves the use of processing functions that transform user input data to a form that is easier or more efficient for the network. For instance, mapminmax processing function transforms input data so that all values fall into the interval [-1, 1]. Also, output processing functions are used to transform user-provided target vectors for network use. These processing functions become part of the trained neural network and influence its outputs in the testing (or utilisation) phase [17].

6.2 Test results

The scheme was tested using frequency deviation data extracted from two hundred and five fault cases. All test cases were predicted successful. Two sample cases involving one stable and one unstable fault case on the line between buses 16 & 21 at base load are presented below to demonstrate the prediction processes of the proposed scheme.

Table 1 shows sampled frequency deviations at the various generator buses in accordance with (8) for a fault on the line between buses 16 and 21 (base load case) which resulted in transient stability. The Table also shows maximum frequency deviation values in accordance with (9). Table 2 on the other hand shows sampled frequency deviations at the various generator buses for the same fault condition but which resulted in transient instability due to delayed fault clearance in line with (8). It also shows maximum frequency deviation values in line with (9).

Table 1. Frequency deviations for line 16-21 stable fault condition

Gen. bus	f_1	f_2	f_{nmax}
1	0.0003	0.0009	0.0009
2	0.0001	0.0006	0.0006
3	0.0003	0.0011	0.0011
4	0.0017	0.0036	0.0036
5	0.0007	0.0019	0.0019
6	0.0011	0.003	0.003
7	0.0012	0.0028	0.0028
8	0.0003	0.0009	0.0009
9	0.0007	0.0017	0.0017
10	0.0001	0.0003	0.0003

Table 2. Frequency deviations for line 16-21 unstable fault condition

Gen. bus	f_1	f_2	f_{nmax}
1	0.0142	0.0154	0.0154
2	0.0153	0.0159	0.0159
3	0.0149	0.0152	0.0152
4	0.0312	0.0308	0.0312
5	0.0321	0.0324	0.0324
6	0.0375	0.0375	0.0375
7	0.0376	0.0382	0.0382
8	0.0142	0.0150	0.0150
9	0.0159	0.0164	0.0164
10	0.0125	0.0134	0.0134

It can be observed from Tables 1 and 2 that the deviations for the unstable case are higher than those for the stable case. The corresponding maximum deviations for the unstable case are thus higher than those for the stable case. These results are representative of results obtained for the other fault conditions simulated.

Applying (10) to the maximum frequency deviation data in Tables 1 and 2, the deviation vector for the stable and unstable cases are obtained as follows:

$$D_{f,stable} = \begin{bmatrix} 0.0009 \\ 0.0006 \\ 0.0011 \\ 0.0036 \\ 0.0019 \\ 0.0030 \\ 0.0028 \\ 0.0009 \\ 0.0017 \\ 0.0003 \end{bmatrix}, D_{f,unstable} = \begin{bmatrix} 0.0154 \\ 0.0159 \\ 0.0152 \\ 0.0312 \\ 0.0324 \\ 0.0375 \\ 0.0382 \\ 0.0150 \\ 0.0164 \\ 0.0134 \end{bmatrix}.$$

Applying (11) to the obtained deviation vectors, the Euclidean norms for the stable and unstable cases are obtained as follows: $d_{stable} = 0.00629126$, $d_{unstable} = 0.07926676$

Putting $x = d_{stable} = 0.00629126$ and $x = d_{unstable} = 0.07926676$ in (1) to (5) together with the application of MATLAB processing functions yields the following MLPNN outputs: $O_{stable} = 0.000017143$, $O_{unstable} = 0.99992$

Finally, applying (6) and (7), the final MLPNN outputs are: $O_{stable} = 0$, $O_{unstable} = 1$

Additional summarized results are presented in Tables 3 and 4. The results presented in Tables 3 and 4 are representative of results obtained for the other fault conditions simulated.

Table 3. Euclidean norms and corresponding MLPNN outputs for stable cases at 80% base loading

Fault	MLPNN output		
	D	Actual	Final
Bus 11	0.0054	0.000017	0
Bus 14	0.0056	0.0000171	0
Bus 21	0.006	0.0000169	0
Bus 24	0.0053	0.0000169	0
Bus 28	0.0049	0.000017	0
Line 5-6	0.0055	0.000017	0
Line 6-7	0.0056	0.0000169	0
Line 6-11	0.0056	0.0000169	0
Line 11-12	0.0053	0.0000169	0
Line 13-14	0.0052	0.0000169	0

Table 4. Euclidean norms and corresponding MLPNN outputs for unstable cases at 80% base loading

Fault	MLPNN output		
	D	Actual	Final
Bus 11	0.0674	0.999919	1
Bus 14	0.0560	0.999918	1
Bus 21	0.0608	0.999919	1
Bus 24	0.0459	0.999901	1
Bus 28	0.0432	0.999879	1
Line 5-6	0.0673	0.999919	1
Line 6-7	0.0683	0.999919	1
Line 6-11	0.0705	0.999919	1
Line 11-12	0.0727	0.999920	1
Line 13-14	0.0664	0.999919	1

The execution time of the proposed scheme is estimated to be 238 ms. This time is made up of 34 ms of input data capture (*ie* two frequency deviation samples at a sampling rate of 60 samples per second), typical wide area measurement (WAM) delay time of 200 ms [19], and algorithm data processing and decision making time of 4 ms (Using Intel(R) Core(TM) i5-3230M CPU @ 2.60 GHz processor). This time compares more favourably with the average algorithm execution time of 700 ms in [5] and 2.5 s algorithm execution time in [9]. Also, using a simple data processing approach, the scheme constructs a single input feature per generator as against 34 features per generator in [7]. For the proposed scheme, the final input to the decision tool is also single, irrespective of the number of system generators. Furthermore, no predetermined templates are required by the proposed scheme, unlike in [5] where a complex simulation process is required to determine generator boundaries.

7 Conclusion

In this paper, a scheme for predicting transient stability status of power systems following disturbances has been presented. The input data required by the scheme can be captured by phasor measurement units which are now deployed in modern power systems. The sampling frequency used in the development of the scheme conforms to the sampling rate of deployed phasor measurements units. The approach to input data processing and decision making is simple. The short window of input data capture coupled with the simple input data processing and decision making approach will enable speedy operation, which is critical. The overall methodology used by the scheme is simple and can be easily inculcated in existing numeral relays. The scheme accurately predicted the stability status of two hundred and five disturbance cases simulated. The scheme is thus highly accurate. Compared

with other schemes in literature, the proposed approach is simpler and easier to implement.

REFERENCES

- [1] T. Rahman, S. Sankaran, N. Seeley and K. Garg, "Capturing Generator Rotor Angle and Field Quantities SDG&E Experience and Approach to Using Nontraditional Generator Measurements", *Proceedings of 42-nd Annual Western Protective Relay Conference, Washington*, 2015.
- [2] A. D. Rajapakse, F. Gomez, O. M. K. K. Nanayakkara, P. A. Crossley, and V. V. Terzija "Rotor Angle Stability Prediction Using Post-disturbance voltage trajectory patterns", *Power & Energy Society General meeting*, pp. 1-6, 2009.
- [3] P. Kundur, J. Paserba, V. Ajjarapu, G. Andersson, A. Bose, C. Canizares, N. Hatziaargyriou, D. Hill, A. Stankovic, C. Taylor, T. V. Cutsem and V. Vittal, "Definition and Classification of Power System Stability", *IEEE Transactions on Power Systems*, vol. 19, no. 2, pp. 1387-1401, 2004.
- [4] N. Amjady and S. F. Majedi, "Transient stability prediction by a hybrid intelligent system", *IEEE Transaction on Power Systems*, vol. 22, no.3, pp. 1275 -1283, 2007.
- [5] D. R. Gurusinge and A. D. Rajapakse, "Post-Disturbance Transient Stability Status Prediction Using Synchrophasor Measurements", *IEEE Transactions on Power Systems*, vol. 31, no.5, pp. 3656-3664, 2016.
- [6] A. N. AL-Masri, M. Z. A. A. Kadir, H. Hizam and N. Mariun, "A Novel Implementation for Generator Rotor Angle Stability Prediction Using an Adaptive Artificial Neural Network Application for Dynamic Security Assessment", *IEEE Transactions on Power Systems*, vol. 28, no.3, pp. 2516-2525, 2013.
- [7] Y. Zhou, J. Wu, Z. Yu, L. Ji and L. Hao, "A Hierarchical Method for Transient Stability Prediction of Power Systems Using the Confidence of a SVM-Based Ensemble Classifier", *Energies*, vol. 9, pp. 1-20, 2016.
- [8] J. Hazra, R. K. Reddi, K. Das, D. P. Seetharam and A. K. Sinha, "Power Grid Transient Stability Prediction Using Wide Area Synchrophasor Measurements", *Proceeding of 3rd IEEE PES Innovative Smart Grid Technologies Europe (ISGT Europe)*, Berlin, pp. 1-8, 2012.
- [9] T. Guo and J. V. Milanović, "On-line Prediction of Transient Stability Using Decision Tree Method - Sensitivity of Accuracy of Prediction to Different Uncertainties", *Proceedings of the IEEE Grenoble PowerTech*, Grenoble, 2013.
- [10] F. Gomez, A. U. Rajapakse and I. Annakkage and Fernando, "Support Vector Machine-Based Algorithm for Post-Fault Transient Stability Status Prediction Using Synchronized Measurements", *IEEE Transactions on Power Systems*, vol. 26, no.3, pp. 1474-1483, 2011.
- [11] J. Q. Zhao, J. Li, X. C. Wu, K. Men, C. Hong and Y. J. Liu, "A novel real-time transient stability prediction method based on post-disturbance voltage trajectories", *Proceedings of the International Conference on Advanced Power System Automation and Protection*, Beijing, pp. 730-736, 2011.
- [12] A. D. Rajapakse, F. Gomez, O. M. K. K. Nanayakkara, P. A. Crossley and V. V. Terzija, "Rotor angle stability prediction using post-disturbance voltage trajectory patterns", *IEEE Transactions on Power Systems*, vol. 25, no.2, pp. 945-956, 2010.
- [13] D. E. Echeverra, J. L. Rueda, J. C. Cepeda1, D. G. Colomé and I. Erlich, "Comprehensive approach for prediction and assessment of power system transient stability real-time", *Proceedings of the 4th IEEE PES Innovative Smart Grid Technologies Europe (ISGT Europe)*, Copenhagen, pp. 1-5, 2013.
- [14] A. Y. Abdelaziz and M. A. El-Dessouki, "Transient Stability Assessment using Decision Trees and Fuzzy Logic Techniques", *I. J. Intelligent Systems and Applications*, vol. 10, pp. 1-10, 2013.
- [15] IEEE Standard for Synchrophasor Measurements for Power Systems, IEEE Std.C37.118.1-2011, December 2011.
- [16] Power System Simulator for Engineers PSSE University Edition, 2016.
- [17] M. H. Beale, M. T. Hagan, H. B. Demuth, Neural Network ToolboxTM, User Guide, MATLAB, R2016b, pp. 3-2 - 3-5, 2016.
- [18] C. K. Özkan and F. S. Erbek, "The Comparison of Activation Functions for Multispectral Landsat TM Image Classification", *Photogrammetric Engineering & Remote Sensing*, vol. 69, no.11, pp. 1225-1234, 2013.
- [19] B. Naduvathuparambil, M. C. Valenti and A. Feliachi, "Communication Delays Wide Area Measurement Systems", *Proceedings of the thirty-fourth Southeastern Symposium on System Theory*, Huntsville, 2002.

Received 14 December 2017